the model of hydrogenic impurities,[13] indicating that radiation due to impurity transitions below the lowest Landau level is dominant.

Second, the variation of output power with sample conductance is nearly linear.[8] Only if the emitter current is sufficiently large do deviations from this behavior occur, which may be due to increasing Landau-level radiation. A total measured radiation power of only 10^{-8} W indicates a predominant nonradiative recombination; the external power efficiency was found to be about 10^{-5}.

I wish to thank Professor Dr. H. W. Pötzl for his interest in my work and many valuable discussions.

[1]Y. Yafet, R. W. Keyes, and E. N. Adams, Phys. Chem. Solids 1, 137 (1956).
[2]R. F. Wallis and H. J. Bowlden, J. Phys. Chem. Solids 7, 78 (1958).
[3]M. v. Ortenberg and G. Landwehr, Phys. Status Solidi (b) 37, K 69 (1970).
[4]D. M. Larsen, J. Phys. Chem. Solids 29, 271 (1968).
[5]G. E. Stillman, C. M. Wolfe, and J. O. Dimmock, in *Proceedings of the Third International Conference on Photoconductivity, Stanford, California, 1969* (Pergamon, New York, 1972), p. 265.
[6]E. H. Putley, J. Phys. Chem. Solids 22, 246 (1961).
[7]R. Mansfield and I. Ahmad, J. Phys. C: Proc. Phys. Soc., London 3, 423 (1970).
[8]I. Melngailis, G. E. Stillman, J. O. Dimmock, and C. M. Wolfe, Phys. Rev. Lett. 23, 1111 (1969).
[9]S. N. Salomon and H. Y. Fan, Phys. Rev. B 1, 662 (1970).
[10]R. Kaplan, J. Phys. Soc. Jap. Suppl. 21, 249 (1966).
[11]D. Kranzer and E. Gornik, Solid State Commun. 9, 1541 (1971).
[12]I. R. Apel, T. O. Poehler, and C. R. Westgate, Appl. Phys. Let. 14, 161 (1969).
[13]E. Burstein and N. Sclar, Phys. Rev. 98, 1757 (1955).

Nonequilibrium Phenomena in Electron Tunneling in Normal Metal-Insulator-Metal Junctions*

P. N. Trofimenkoff, H. J. Kreuzer, W. J. Wattamaniuk, and J. G. Adler
Department of Physics, University of Alberta, Edmonton, Canada
(Received 15 May 1972)

Structure in the conductance of normal metal-insulator-metal junctions at very low bias is explained through a nonequilibrium treatment of the tunneling process. In particular, the related peak in the derivative $d\sigma(V)/dV$ is quantitatively accounted for by the blocking of otherwise available electron tunneling states due to the finite electron relaxation rates in the metal electrodes.

A great deal of effort has been devoted to the theoretical and experimental study of low-bias structure in the dynamic conductance $\sigma = dI/dV$, and its derivative $d\sigma/dV$, of normal metal-insulator-metal tunneling junctions.[1] This Letter deals with the very small conductance minima in the vicinity of zero bias and below the phonon peaks[2] that have been observed for a variety of combinations of metal electrodes.[3] Our attention is focused on the very small zero-bias structure rather than the large magnetic zero-bias anomalies[1] or the effect of metallic inclusions in the insulating film.[4] We consider the nonequilibrium aspects of tunneling and present a transport model that explains the very small structure which occurs near zero bias.

In the usual semiclassical single-particle-transfer picture, tunneling is restricted to electrons with momenta in the forward direction (perpendicular to the barrier) and is assumed to occur between equilibrium electron distributions in the metal electrodes on either side of the barrier. In the presence of a current a nonequilibrium situation exists, and the electron relaxation rates

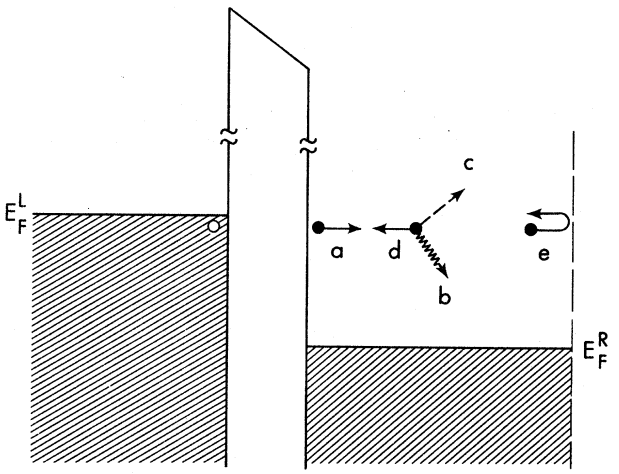

FIG. 1. Schematic diagram of scattering processes described in the text.

in the metal electrodes have to be taken into account.

With reference to Fig. 1, an electron that tunnels through the barrier will leave a hole in the left electrode and occupy a state a in the right electrode. This electron will travel away from the barrier in the right electrode and may be scattered through various mechanisms: (1) Inelastic scattering with emission or absorption of a phonon, b, will alter both the electron's energy and momentum; this type of process will be described by an energy- and temperature-dependent relaxation time $\tau_{ep}(E, T)$, where E is the energy measured relative to the chemical potential of the right electrode and T is the temperature. (2) Elastic scattering by impurities, c,d, will alter the electron's momentum only and will be accounted for by a constant relaxation time τ_i. (3) Boundary scattering, if specular, e, will reverse the component of the electron's momentum perpendicular to the barrier. The specular boundary scattering at the electrode extremities leads to a stationary picture with relaxation times $\tau_{ep}(E, T)$ and τ_i to describe scattering of electrons out of the forward direction. Additionally, since electrons with momenta in the forward direction dominate the current, it is suitable to consider the energy variable alone without the complications of the momenta.

For the stationary model described above the following two rate equations hold in the steady state in the right (R) and left (L) electrodes:

$$\frac{\partial f_R(E,T)}{\partial t} = 0 = \frac{D}{\tau_0}[f_L(E,T) - f_R(E,T)] - \delta f_R(E,T)\left[\frac{1}{\tau_{ep}^{R}(E,T)} + \frac{1}{\tau_i^{R}}\right], \tag{1a}$$

$$\frac{\partial f_L(E,T)}{\partial t} = 0 = -\frac{D}{\tau_0}[f_L(E,T) - f_R(E,T)] - \delta f_L(E,T)\left[\frac{1}{\tau_{ep}^{L}(eV-E)} + \frac{1}{\tau_i^{L}}\right], \tag{1b}$$

where $f_L(E,T) = f_0(E - eV, T) + \delta f_L(E,T)$ and $f_R(E,T) = f_0(E,T) + \delta f_R(E,T)$ are the steady-state occupations in the left and right electrodes as opposed to the equilibrium distributions $f_0(E - eV, T)$ and $f_0(E,T)$, D is the intrinsic constant barrier penetrability, and $1/\tau_0$ is the decay constant, so that D/τ_0 is a transition rate for electrons crossing the barrier.

Equations (1a) and (1b) are interpreted as follows. In the steady state the change of occupation with time in the right and left electrodes is zero. The first term on the right-hand side of Eq. (1a) describes the net flow of electrons into states of energy E in the right electrode; the second term describes the scattering out of these states. In Eq. (1b) the first term on the right-hand side describes the loss of occupation in the left electrode and the second term describes the decay of holes; the hole relaxation rate is taken to be symmetric with the electron relaxation rate about the Fermi level in the left electrode.

Solution of Eqs. (1a) and (1b) provides

$$f_L(E,T) - f_R(E,T) = [f_0(E - eV, T) - f_0(E,T)][1 - g(E)], \tag{2a}$$

where the blocking factor $g(E)$ is given by

$$g(E) = \frac{D/\tau_0}{D/\tau_0 + [\tau_L(eV - E, T) + \tau_R(E,T)]^{-1}}, \tag{2b}$$

where $\tau^{-1} = \tau_{ep}^{-1} + \tau_i^{-1}$. In the calculation of the current I, σ, and $d\sigma/dV$, the above expression for $f_L(E,T) - f_R(E,T)$ is to be used rather than $f_0(E - eV, T) - f_0(E,T)$. The consequences of the additional blocking factor will be made explicit below.

The electron-phonon relaxation time $\tau_{ep}(E,T)$ is given by Fermi's "golden rule" to be[5]

$$[\tau_{ep}(E,T)]^{-1} = (2\pi/\hbar)\int_0^{\omega_0} d\omega\, \alpha^2(\omega)F(\omega)[2N_0(\omega,T) + 1 - f_0(E-\omega,T) + f_0(E+\omega,T)], \tag{3}$$

where $\alpha^2(\omega)F(\omega)$ is the product function involving the electron-phonon coupling function and the phonon density of states $F(\omega)$ [$F(\omega) = 0$ for $\omega > \omega_0$], and $N_0(\omega,T)$ is the equilibrium distribution function for the phonons.

Experimentally, the zero-bias structure is observed in a region up to 1 or 2 mV, and the maximum change in σ is $\cong 0.1\%$. At $E = 1$ meV in Al, $\tau_{ep}(1\text{ meV}, T = 0^\circ\text{K}) \cong 10^{-10}$ sec. The time τ_0 is equated to $2l/v_F$, where l is the electrode thickness and v_F is the Fermi velocity, to obtain $\tau_0 \cong 2\times 10^{-13}$ sec for $l = 2000$ Å. D is obtained from $g(E) \cong 10^{-3}$ to be $\cong 2\times 10^{-6}$ if the impurity time τ_i is equated to the electron-phonon time τ_{ep}. This value of D corresponds to a current density $\cong 30$ mA/mm^2 at 1 mV, which,

for a 50-Ω junction and a tunneling current of 0.02 mA at 1 mV, leads to an effective tunneling area $\cong 10^{-3}$ mm^2.

The implications of the blocking term in Eq. (2a) on σ and $d\sigma/dV$ can readily be understood if the case where the left-electrode electron distribution is considered to be in equilibrium ($\tau_L = 0$). Since D/τ_0 is appreciably less than $1/\tau(E)$, it can be neglected in the denominator of the blocking factor $g(E)$. For the case $T = 0$°K and $\alpha^2(\omega)F(\omega)$ linear in the relevant low-energy region [$\alpha^2(\omega)F(\omega) = \alpha^2\omega$, α^2 a constant], one obtains

$$\sigma(V) \propto D\ 1 - \left[\frac{D/\tau_0}{1/\tau_i + (\pi/\hbar)\alpha^2(eV)^2}\right], \tag{4a}$$

$$\frac{d\sigma(V)}{dV} \propto \frac{(D^2/\tau_0)\alpha^2(eV)}{[1/\tau_i + (\pi/\hbar)\alpha^2(eV)^2]^2}. \tag{4b}$$

The features of these expressions are (1) the narrow minimum in $\sigma(V)$ of Eq. (4a) at zero bias, and (2) the rise of $d\sigma(V)/dV$ at low bias and its pronounced peaking behavior. The above simple case with $T = 0$°K and one electrode in equilibrium reproduces the qualitative features of the experimental data.

For a quantitative comparison with our Al-Al$_x$O$_y$-Al data both electrodes have to be taken into account. The results for temperature T and $\tau_i^L = \tau_i^K$ are

$$\frac{\sigma(V)}{\sigma(0)} = 1 - \frac{D}{\tau_0}\int_{-\infty}^{\infty}\frac{dE}{kT}\frac{e^{-(E-eV)/kT}}{[e^{-(E-eV)/kT}+1]^2}[\tau_L(-E)+\tau_R(E)], \tag{5a}$$

$$\frac{1}{\sigma(0)}\frac{d\sigma(V)}{dV} = \gamma\int_0^{\infty}dx\frac{e^x}{(e^x+1)^2}[S(eV-xkT)+S(eV+xkT)], \tag{5b}$$

where $S(E) = E/[E^2 + (\pi kT)^2 + \delta]^2$, $\gamma = 4D\hbar e/\pi\tau_0\alpha^2$, and $\delta = \hbar/\pi\tau_i\alpha^2$.

Figure 2 shows the experimental curves of $d\sigma_e(V)/dV$ [which is the even part of $d\sigma(V)/dV$, used to avoid any difficulties due to asymetries of the background] versus V for an Al-Al$_x$O$_y$-Al junction measured at $T = 3.0$, 4.1, 5.0, and 6.0°K.[6] The dashed line is the theoretical curve of Eq. (5b) fitted to the 3.0°K data to obtain $D/\tau_0 = 0.72 \times 10^7$ sec^{-1} and $\tau_i = 3.5 \times 10^{-10}$ sec. The overall shape of the curves is not extremely sensitive to temperature. Accordingly, the theoretical and experimental peak positions and heights are compared in Fig. 3. Excellent agreement is found for the peak positions as a function of temperature. The theory predicts a stronger temperature dependence for the peak heights than is experimentally observed. However, it must be noted that the details of the overall fit, and temperature dependence of the peak position and

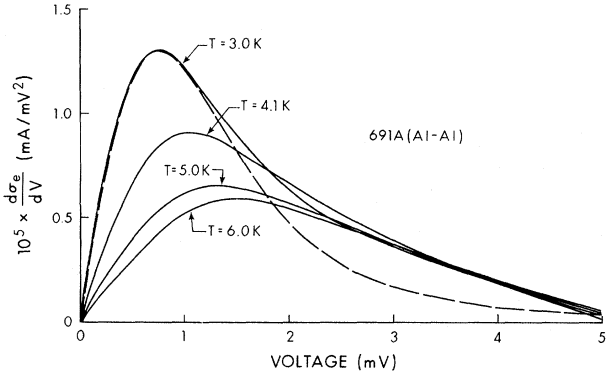

FIG. 2. Even part of $d\sigma/dV$ as a function of V for different temperatures. Solid lines, experimental data; dashed line, theoretical result for $T = 3$°K.

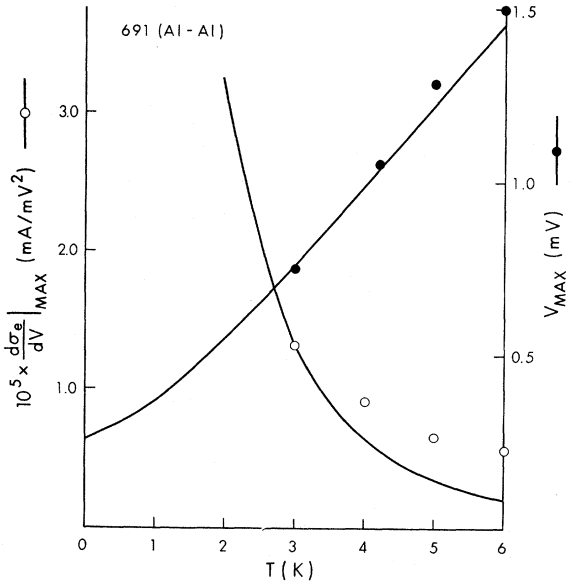

FIG. 3. Plot of maximum height $(d\sigma_e/dV)_{max}$ and position V_{max} of peak as a function of temperature. Solid curves, theoretical results obtained using the fit of D/τ_0 and τ_i (see text) to the $T = 3$°K points.

magnitude, will depend on the detailed form of the low-energy behavior of $\alpha^2(\omega)F(\omega)$. For the theoretical calculations given here, $\alpha^2(\omega)F(\omega)$ has been chosen to be linear in ω for reasons of simplicity[7]; the choice $\alpha^2(\omega)F(\omega) = \alpha^2\omega^2$ would not affect the general conclusions.

In conclusion, the observed structure near zero bias in the conductance σ and its derivative $d\sigma/dV$ for normal metal-insulator-metal tunneling junctions has been accounted for by including the effects of finite electron relaxation rates in the junction electrodes. The nonzero lifetimes lead to an observable blocking of otherwise-available electron tunneling states at low bias.

*Work supported in part by grants from the National Research Council of Canada.

[1]See, for example, the review by C. B. Duke, *Tunneling in Solids*, Suppl. 10 to *Solid State Physics*, edited by F. Seitz, D. Turnbull, and H. Ehrenreich (Academic, New York, 1969).

[2]J. Lambe and R. C. Jaklevic, Phys. Rev. 165, 821 (1968); J. M. Rowell, W. L. McMillan, and W. L. Feldmann, Phys. Rev. 180, 658 (1969).

[3]T. T. Chen and J. G. Adler, Solid State Commun. 8, 1965 (1970).

[4]H. R. Zeller and I. Giaever, Phys. Rev. 181, 789 (1969).

[5]See, for example, J. W. Wilkins, *Observable Many Body Effects in Metals* (Nordita, Copenhagen, 1968).

[6]These measurements were obtained by standard high-resolution spectroscopy methods; see, for example, J. G. Adler, T. T. Chen, and J. Straus, Rev. Sci. Instrum. 42, 362 (1971).

[7]A calculation of $\alpha^2(\omega)F(\omega)$ using one orthogonalized plane wave gives a linear low-energy behavior; see, e.g., J. P. Carbotte and R. C. Dynes, Phys. Rev. 172, 476 (1968). Because of band-structure effects it is not expected that $\alpha^2(\omega)F(\omega)$ remains linear in the very low-energy region. We have used $\alpha^2 = 3\times10^{-3}$ meV^{-1}.

Magnetoplasma Surface Waves in Polar Semiconductors: Retardation Effects*

K. W. Chiu and J. J. Quinn†
Brown University, Providence, Rhode Island 02912, and Max-Planck-Institut für Festkörperforschung, Stuttgart, Germany
(Received 19 June 1972)

Full dispersion curves, including the effect of retardation, are presented for the coupled optical-phonon–magnetoplasmon surface waves of a degenerate polar semiconductor. The dispersion curves display a surprising amount of interesting new structure which does not occur in the absence of a dc magnetic field.

The effect of a dc magnetic field on the dispersion relation of surface plasmons in solids has recently received considerable theoretical attention.[1-3] For a completely arbitrary magnetic field, the dependence of the surface-plasmon frequency on the magnitude and orientation of the applied field has been given[2] for the nonretarded limit in which the phase velocity ω/q is small compared with the speed of light c. The full dispersion curve, including the effect of retardation, has been studied for particular cases in which the applied field is either parallel or perpendicular to the surface.[1] Recently, Brion *et al.*[3] have reinvestigated one of the cases studied in Ref. 1, that of magnetoplasma surface-wave propagation perpendicular to a dc magnetic field which is oriented parallel to the surface. They found that gaps appear in the dispersion relation if the background dielectric constant ϵ_L satisfies the inequality $\epsilon_L^2 > 1 + \epsilon_L^{-1}\omega_c^{-2}\omega_p^2$, where $\omega_p = (4\pi ne^2/m)^{1/2}$ is the bulk plasma frequency.

In all of these papers the background dielectric constant was considered to be independent of frequency. For polar semiconductors, however, the background dielectric constant is not independent of frequency, but is given by

$$\epsilon_L(\omega) = \frac{\epsilon_\infty\omega^2 - \epsilon_0\omega_T^2}{\omega^2 - \omega_T^2}, \tag{1}$$

where ϵ_∞ and ϵ_0 are the high- and low-frequency dielectric constants, and ω_T is the transverse-optical-phonon frequency. By taking into account this frequency dependence of ϵ_L, the surface plasmons and surface optical phonons are found to couple with each other.[4] This interaction has been the object of several recent experimental studies.[5] In the present paper, we generalize our earlier investigations[1,2] to include the effects of phonon coupling on the magnetoplasma surface waves. Full dispersion curves for the coupled modes, including the effect of retardation, are given for different values of the experimen-